A highly discriminatory RNA strand-specific assay to facilitate analysis of the role of *cis*-acting elements in foot-and-mouth disease virus replication

Samuel J. Dobson, Morgan R. Herod, David J. Rowlands, Nicola J. Stonehouse

School of Molecular and Cellular Biology and Astbury Centre for Structural Molecular Biology, Faculty of Biological Sciences, United Kingdom

Abstract

Foot-and-mouth-disease virus (FMDV), the etiological agent responsible for foot-and-mouth disease (FMD), is a member of the genus *Aphthovirus* within the *Picornavirus* family. In common with all picornaviruses, replication of the single-stranded positive-sense RNA genome involves synthesis of a negative-sense complementary strand that serves as a template for the synthesis of multiple positive-sense progeny strands. We have previously employed FMDV replicons to examine viral RNA and protein elements essential to replication, however, the factors affecting differential strand production remain unknown. Replicon-based systems require transfection of high levels of RNA, which can overload sensitive techniques such as qPCR preventing discrimination of specific strands. Here, we describe a method in which replicating RNA is labelled *in vivo* with 5-ethynyl uridine. The modified base is then linked to a biotin tag using click chemistry, facilitating purification of newly synthesised viral genomes or anti-genomes from input RNA. This selected RNA can then be amplified by strand-specific qPCR, thus enabling investigation of the consequences of defined mutations on the relative synthesis of negative-sense intermediate and positive-strand progeny RNAs. We apply this new approach to investigate the consequence of mutation of viral *cis*-acting replication elements and provide direct evidence for their roles in negative-strand synthesis.

Keywords

Foot-and-mouth disease virus; FMDV; replication; strand-specific assay; negative sense; cre

Introduction

The *Aphthovirus* foot-and-mouth disease virus (FMDV) is a member of the *Picornaviridae* family of single-stranded positive sense RNA viruses. FMDV is the etiological agent of foot-and-mouth disease (FMD) and comprises six serotypes; A, O, Asia 1, Southern African Territories (SAT) 1, SAT 2 and SAT 3,

29 which are together responsible for endemic infection in large parts of Africa, Asia and the Middle East
30 (1). Whilst FMD is rarely fatal, its consequences of reduced animal productivity, restriction of trade
31 and slaughter of infected and at-risk animals result in severe economic losses (2, 3). The threat to
32 maintenance of virus-free status in non-endemic regions is exacerbated by the high transmissibility of
33 FMDV. Control measures following introduction of FMD into non-endemic regions, including strict
34 movement restriction and mass culling, can result in costs of £billions (3-5). The antigenic diversity of
35 FMDV adds to the challenges of disease control, with little cross-protection provided by strain-specific
36 vaccines and no effective therapeutics currently available (2, 6-10). There is therefore a need to better
37 understand the viral lifecycle in order to develop novel methods of control.

38 The genome of FMDV is approximately 8.4 kb and encodes a single polyprotein that is processed by
39 viral proteases to generate the proteins required for genome replication and encapsidation. Primary
40 cleavage of the polyprotein occurs at three positions to generate four products, the leader protease
41 (L^{pro}), the viral structural protein precursor P1-2A and the non-structural protein precursors P2 (2BC)
42 and P3 ($3AB_{1,2,3}CD$). Cleavage of L^{pro} occurs auto-catalytically, while release of the P1-2A precursor
43 from the polyprotein occurs through a co-translational 2A-dependent ribosome skipping mechanism.
44 The P1-2A region contains the viral structural proteins VP1, VP3 and VP0 (which is cleaved into VP2
45 and VP4 during virion maturation). Subsequent processing of the P2 and P3 precursors generates the
46 viral non-structural proteins 2B, 2C and 3A, $3B_{1,2+3}$ (VPg), 3C protease ($3C^{pro}$) and 3D polymerase ($3D^{pol}$)
47 (11-21). This processing is thought to be mediated by $3C^{pro}$ through alternative *cis*- and *trans*-
48 pathways that appear to co-ordinate replication (17, 22, 23).

49 The single viral open reading frame (ORF) is flanked by untranslated regions (UTRs) at the 5' and 3'
50 ends of the genome. The FMDV 5' UTR is longest amongst known picornaviruses and contains several
51 highly structured domains that are essential to the virus lifecycle (24-30). The S fragment is a ~360
52 nucleotide hairpin-loop that occupies the same location (at the extreme 5' end of the 5' UTR) as the
53 cloverleaf found in enteroviruses (31-34). It appears to be involved in immune modulation and viral
54 replication via interactions with host and viral proteins (27, 35, 36). Adjacent to the S-fragment is a
55 poly-C sequence of unknown function, followed by two to four RNA pseudoknots, which appear to be
56 involved in assembly of infectious virions in addition to genome replication (24, 37-39). Adjacent to
57 the pseudoknots is a small hairpin-loop known as the *cis*-acting replication element (*cre*) that in other
58 picornaviruses is located within the ORF (25, 40). Whilst the location of the *cre* appears not important,
59 it has an indispensable role in replication (25), acting as a template for the uridylylation of VPg by $3D^{pol}$
60 (41-43). VPg_pU_pU primes genome replication by $3D^{pol}$ (22, 44, 45). Finally, the internal ribosome entry

61 site (IRES) is located immediately upstream of the ORF and is essential for initiation of translation (26,
62 29, 30, 46).

63 Picornavirus genome replication is initiated by the synthesis of a negative-sense copy of the infecting
64 genome followed by assembly of a 'replicative form' (47-49). This complex comprises the negative
65 strand template RNA and several nascent progeny positive strand RNAs together with $3D^{pol}$ and other
66 viral and cellular proteins (50, 51). There is evidence that in the native state of the replicative form the
67 nascent daughter strands are not collapsed onto the negative template strand but are only transiently
68 associated at the site of transcription (50). The synthesis of both negative and positive RNA strands
69 appears to be primed with VPg_pU_pU (41).

70 While it is well documented that the *cre* element is essential for viral replication, it is not firmly
71 established whether this is required to produce VPgpUpU for the priming of both negative- and
72 positive-sense RNA molecules during intra-cellular virus replication. Indeed, it has been reported that
73 priming of negative-strand RNA synthesis can occur in a *cre*-independent manner during cell-free
74 replication of poliovirus, possibly via the poly(A) tail (52-54). As mutation of the *cre* is lethal to progeny
75 virus production, methods that facilitate the initiation of replicative events but are not reliant on
76 infection (such as transfection of *in vitro* transcribed viral RNA) are useful for study of the initial steps
77 in replication. Whilst assays to distinguish positive- and negative-strand RNAs have been developed
78 for several viruses including FMDV, o'nyong-nyong virus, dengue virus, murine norovirus and
79 chikungunya virus, their applications have so far been limited to studies involving infectious virus
80 production (55-59).

81 Replicons are mini-genomes in which the structural genes are replaced with a reporter gene to
82 facilitate the study of RNA replication independent of other aspects of the virus lifecycle (60). In
83 addition to their application in the dissection of the molecular details of replication, replicons permit
84 the study of viruses that require high-containment facilities, such as FMDV, at lower laboratory
85 containment. However, because the delivery of RNA by transfection is an inefficient process, large
86 quantities of *in vitro* transcribed RNA are used in order to ensure that sufficient cells are transfected.
87 This can overload subsequent strand-specific assays. Here, we describe a strand-specific qPCR assay
88 using FMDV replicons to determine the effects of mutations on the synthesis of both negative and
89 positive strands. We have applied this method to determine the role of the *cre* element in the initiation
90 of synthesis of both positive- and negative-strand RNAs.

91

92 ## Materials and methods

93 ### Cell lines and maintenance

94 Baby hamster kidney (BHK-21) cells were purchased from ATCC (LGC Standard) and were maintained
95 in Dulbecco's modified Eagle's medium (DMEM) with glutamine, supplemented with 10% (v/v) foetal
96 bovine serum (FBS), 50 U/mL penicillin and 50 µg/mL streptomycin. Growth medium and supplements
97 were purchased from Sigma-Aldrich, Merck.

98 ### *In vitro* transcription

99 The construction, linearisation and purification of FMDV replicon plasmids has been described
100 previously (24, 60). Linear plasmids were transcribed *in vitro* using the T7 RiboMAX Express Large Scale
101 RNA Production System (Promega) using 'half sized' reactions whereby 250 ng linear plasmid was
102 added to a reaction mixture using half the volume suggested for all reagents in the manufacturer's
103 protocol. Reactions were incubated at 37°C for 1.5 hours prior to addition of 1 µL DNase I and further
104 incubation at 37°C for 20 minutes. Resulting RNA was purified using the RNA Clean & Concentrator-
105 25 kit (Zymo Research) prior to quantification by NanoDrop (Thermo Fisher) and confirmation of
106 integrity by denaturing MOPS-formaldehyde gel electrophoresis.

107 ### Replication assays

108 BHK-21 cells were seeded into 6-well plates at a density of $1X10^6$ cells/well and incubated for 16 hours.
109 After incubation, cells were transfected with *in vitro* transcribed replicon RNA using Lipofectamine
110 2000 (Thermo Fisher). RNA (0.5 $\mu g/cm^2$) and Lipofectamine 2000 (1 µg RNA:3 µL reagent) were added
111 separately to 50 µL opti-MEM (Thermo Fisher) and incubated for 10 minutes at room temperature.
112 RNA and reagent were mixed and incubated for 20 minutes at room temperature before diluting with
113 phenol red free DMEM (Thermo Fisher) supplemented with 10% (v/v) FBS and GlutaMAX (Thermo
114 Fisher) diluted to 1x. Cells were washed 1x using PBS, before addition of transfection mixture. Cells
115 were imaged over time using the 10X objective of an Incucyte S3 live cell imaging system to detect
116 phase and green fluorescence. Analysis was performed with the inbuilt Incucyte 2021A analysis suite
117 using surface fit segmentation, threshold minimum (green calibrated units, GCU) 8.0, edge split
118 sensitivity -30, minimum area filter 50 μm^2 to determine green fluorescent cells. Following incubation
119 for 6 hours, cells were washed 1x with PBS and extracted by addition of 1 mL TRI reagent (Merck)
120 directly to the monolayer. Harvested cell extracts were stored at -20°C until further processing.

121 **RNA extraction and cDNA synthesis**

122 Total RNA was TRI reagent extracted from BHK-21 cells using Phasemaker tubes (Invitrogen, Thermo
123 Fisher) and associated manufacturer protocol. An additional 75% EtOH RNA pellet wash step was
124 performed to ensure removal of trace contaminants prior to RNA solubilisation using nuclease-free
125 H_2O. Contaminating DNA was removed using the TURBO DNA-*free* kit (Thermo Fisher) following
126 manufacturer guidelines. Total RNA purity and concentration was determined by NanoDrop.

127 cDNA synthesis was performed using SuperScript IV Reverse Transcriptase (Thermo Fisher) following
128 manufacturer guidelines unless stated otherwise. Separate reactions were performed using 2 µM
129 strand-specific reverse transcription (ssRT) primer (Table 1, PS-tag-RT or NS-tag-RT) or 50 µM
130 oligo$(dT)_{20}$. A total mass of 500 ng RNA was added to each reaction, together with dNTP mix containing
131 10 mM of each nucleotide (Promega). Combined reaction mixtures were incubated at 50°C for 10
132 minutes prior to inactivation at 85°C for 10 minutes.

133 **qPCR assays**

134 cDNA synthesised from total RNA was diluted 100-fold in nuclease-free H_2O unless otherwise stated.
135 qPCR was performed using GoTaq qPCR Master Mix (Promega). Reaction mixes were made up in 10
136 µL total volume containing 500 nM forward and reverse primers (Table 1, PS-qPCR-tag & PS-qPCR-R
137 or NS-qPCR-tag & NS-qPCR-R or β-actin-F & β-actin-R) and 2 µL diluted cDNA. qPCR conditions
138 followed the manufacturer recommended fast cycling program with polymerase activation (95°C, 2
139 minutes) followed by 40 cycles (denaturation at 95°C, 3 seconds and annealing/extension at 60°C, 30
140 seconds) with melt curve analysis on a CFX Connect Real-Time PCR Detection System (Bio-Rad).

141 **Nascent RNA labelling assays**

142 Nascent RNA labelling assays were performed using the Click-iT™ Nascent RNA Capture Kit (Thermo
143 Fisher). Replication assays were performed as described previously in 6-well plates, with addition of
144 0.2 mM 5-ethynyl uridine (5-EU) diluted from a 200 mM stock, to transfection complex mixtures
145 immediately prior to addition to cells. Cells were harvested 6 hours post transfection through the
146 addition of 1 mL TRI reagent (Sigma-Aldrich, Merck) directly to the monolayer, with collected samples
147 stored at -20°C until further processing. RNA was extracted as indicated above. Biotinylation of RNA
148 by click reaction was performed following manufacturer guidelines using 10 µg total RNA and 0.5 mM
149 biotin azide in a 50 µL reaction. RNA was precipitated in ammonium acetate overnight at -80°C,
150 pelleted, washed and solubilised in nuclease-free H_2O, as recommended. RNA was quantified by
151 NanoDrop and 1 µg biotinylated RNA mixed with 12 µL Dynabeads® MyOne™ Streptavidin T1 magnetic
152 beads. Following 30 minutes incubation at room temperature with agitation at 600 rpm, beads were

153 washed for 3 minutes at room temperature with agitation at 600 rpm 5x using washer buffer 1 and 5x
154 using wash buffer 2, with magnetic capture performed between washes. Bead mixtures were
155 transferred to a new tube after every three washes to minimise tube contaminant carry over.
156 Following the final wash, beads were resuspended in 36 µL wash buffer 2 and 12 µL slurry divided
157 between three separate tubes for separate reverse transcription of positive-strand genomes,
158 negative-strand genomes and total poly(A) RNA. Bead suspensions were heated at 70°C for 5 minutes
159 prior to immediate addition of 17 µL master mix containing 15 µL NF-H_2O, 1 µL 10 mM dNTPs and 1
160 µL 2 µM ssRT primer (Table 1) or 50 µM Oligo$(dT)_{20}$. Mixes were cooled to room temperature with
161 agitation at 600 rpm for 10 minutes before addition of 8 µL 5x SuperScript IV reaction buffer, 2 µL 100
162 mM DTT and 1 µL SuperScript IV enzyme to each reaction. Samples were incubated at 50°C for 1 hour
163 with agitation at 600 rpm. Reaction mixtures were heated at 85°C for 10 minutes to inactivate reverse
164 transcription and release cDNA from beads. Tubes were pulse centrifuged to pellet liquid prior to bead
165 immobilisation using a magnetic rack and aspiration of cDNA. cDNA was diluted 100-fold for positive-
166 strand reactions and 10-fold for negative-strand reactions. Oligo$(dT)_{20}$ reactions were diluted
167 accordingly. qPCR reactions were performed as previously described above with quantification using
168 the ΔΔCq method. Samples in which no signal was detected were arbitrarily assigned a C_T value of 40
169 to permit quantification.

170

171 ## Results

172 **Transfection with replicon RNA is not compatible with strand-specific discrimination by qPCR.**

173 Reverse genetics is a powerful tool for investigating the molecular biology of many viruses. However,
174 a common drawback with many reverse genetics systems is the inefficient delivery of *in vitro*
175 transcribed viral genomes, which can overwhelm assays deigned to dissect individual steps of viral
176 lifecycles such as strand-specific genome synthesis. To overcome this restriction we have developed
177 assays involving nascent RNA labelling, reverse transcription and strand-specific qPCR to examine the
178 individual steps of negative- and/or positive-strand synthesis.

179 Our previously reported assays of replication utilised a FMDV replicon encoding the GFP reporter
180 protein in place of the viral structural proteins (60, 61). Transfection of *in vitro* transcribed replicon
181 RNA into cells allows measurement of a completed replication cycle via GFP expression prior to RNA
182 extraction, cDNA synthesis and measurement of strand-specific specific RNA replication by qPCR
183 (Figure 1A). Following transfection with *in vitro* transcribed pRep-ptGFP replicon RNA (WT or the
184 replication-deficient $3D^{GNN}$) or yeast tRNA (as a control), cells were examined using an Incucyte S3

185 instrument to visualise phase contrast and green images (representative images Figure 1B) and the
186 number of ptGFP positive cells determined using pre-defined analysis parameters (Figure 1C).

187 Strand-specific primers with a non-viral tag sequence were designed for use during reverse
188 transcription reactions to generate unique 5' sequences providing specificity for each strand (Table 1)
189 similar to published protocols (55-58). In order to minimise the potential for cross-contamination,
190 primers were designed towards the 5' and 3' ends of the FMDV replicon genome for the positive-
191 strand and negative-strand, respectively (Figure 1D). Reverse transcription using oligo$(dT)_{20}$ was also
192 performed for each sample to permit normalisation between samples by amplifying β-actin as a stably
193 expressed reference gene. A primer complementary to the strand-specific non-viral tag and an
194 internal primer complementary to the viral genome were designed for the strand-specific qPCR. Initial
195 assays were performed comparing strand production between WT and $3D^{GNN}$ replicons. As
196 anticipated, only a ≈2 fold-difference was observed between WT and $3D^{GNN}$ for both strands (Figure
197 1E&F), suggesting that the ability to demonstrate nascent viral RNA production was masked by the
198 large quantity of input RNA necessary to efficiently initiate replication.

199 **Removal of input replicon genomes by nascent RNA labelling.**

200 We speculated that the inability of the strand-specific qPCR to distinguish between RNA isolated from
201 cells transfected with either replication-competent or -incompetent replicon constructs was due to
202 the large amount of input RNA necessary to initiate replication in the majority of the cells. To address
203 this, we developed a method to specifically label and isolate newly synthesised RNA. To facilitate
204 selection, transfected cells were incubated with an alkyne-modified uridine, 5-EU, from the time of
205 transfection so that only cellular RNAs and viral genomes synthesised during replication incorporated
206 the modified nucleotide (Figure 2A). Control assays indicated that addition of 0.2 mM 5-EU to the
207 culture medium did not inhibit replication (Figure 2B).

208 Following RNA extraction, strand-specific qPCR was performed to determine whether incorporation
209 of 5-EU had any adverse effects upon the assay. These assays showed that detection of positive-strand
210 and negative-strand genomes (Figure 2C&D, respectively) was comparable to that observed without
211 labelling (Figure 1E&F). Copper-catalysed click reactions were performed to covalently link azide-
212 modified biotin to the newly synthesised RNA. This acted as a bait for capture with streptavidin
213 magnetic beads and removal by washing of input replicon RNA. Following capture and on-bead reverse
214 transcription, analysis of the eluted cDNA confirmed that the method had efficiently removed replicon
215 input RNA, with the $3D^{GNN}$ replicon signal reduced to 0.03 and 0.02 of WT for positive-strand and
216 negative-strand, respectively (Figure 2E&F). This confirmed that labelling of newly synthesised RNA

217 with 5-EU prior to biotin modification by click reaction and bead capture provided a method suitable
218 for replicon-based investigation of differential viral strand synthesis.

219 ***Cre* is essential for negative-strand production.**

220 The *cre* is essential to replication of picornaviruses by acting as a template for uridylylation of VPg by
221 $3D^{pol}$. There is also evidence that the poly(A) tail of poliovirus may act as a template for uridylylation
222 in cell-free replication, albeit-it less efficiently (52-54). However, whether c*re* is essential for VPg
223 uridylylation to prime the negative-strand intermediate during replication in cells is unknown. The role
224 of the c*re* in strand synthesis was therefore investigated using replicons harbouring a complete c*re*
225 deletion (Δ*cre*) or with a single nucleotide substitution of the functional AAACA motif (termed A1G,
226 containing mutation of the first A nucleotide to G). Both of these mutations are known to prevent the
227 complete virus lifecycle (25). Loss of replication competency was confirmed here for both mutants by
228 replicon assay (Figure 3A). Strand-specific assays confirmed that the positive-strand could not be
229 synthesised by either mutant replicon (Figure 3B). Negative-strand production was also ablated,
230 showing that the c*re* is also essential during intracellular replication for production of the negative-
231 strand (Figure 3C).

232 Discussion

233 The ability to reliably differentiate positive-strand and negative-strand RNAs is important for
234 investigating details of the mechanism of picornavirus replication. This can be achieved using qPCR
235 techniques, but the selection of strand-specific primers can be challenging. This problem is
236 exacerbated when studying replicons, as reliable transfection requires a large quantity of input RNA.
237 Despite these drawbacks, replicons facilitate investigations of replication that would otherwise be
238 technically challenging, e.g. with non-recoverable or poorly replicating viruses, or to address issues
239 regarding containment and safety. We therefore designed a strand-specific qPCR assay to distinguish
240 synthesis of each strand separately and explored how mutation to the viral genome may restrict
241 synthesis.

242 Initial assays identified the large quantity of input RNA required to ensure transfection of the majority
243 of cells as a major restriction to demonstrating differences between replication-competent and -
244 defective replicons (Figure 1). In the case of the FMDV replicon, the ≈ 7 kb genome relates to
245 approximately 1.8×10^{12} genome copies/µg, and with up to 5 µg/well of replicon being transfected
246 into cells, carry-over of input RNA was unsurprising. RNA self-priming, a consequence of high
247 secondary structure at the 3' terminus of RNA and reverse transcriptases lacking RNase H activity, has
248 been reported previously as a source of contamination by complementary sequences in strand-

249 specific assays (57, 58). In addition, residual fragments of plasmid DNA used as template for *in vitro*
250 transcription of the transfecting RNA could theoretically also be a source of contaminating
251 complementary sequences. However, contamination by any interfering sequences is eliminated by
252 the specific selection of newly synthesised RNA as described here, thus providing an assay that can
253 reliably distinguish complementary strands.

254 The essential role of the *cre* in picornavirus replication is well documented and was also confirmed
255 here in replicon assays (Figure 3A) (36, 52-54, 62). It is possible that the poly(A) tail could template
256 uridylylation of VPg (i.e. in addition to and independently of the c*re*, as reported in cell-free assays)
257 (52-54). However, it was not established whether the c*re* is required for negative-strand synthesis in
258 an intracellular assay. We therefore investigated the role of two c*re* mutations (A1G and Δ*cre*) during
259 strand synthesis and found that neither positive- nor negative-strand RNAs were transcribed. Given
260 that negative-strand intermediates were not produced, it is unsurprising that positive-strand
261 production was also restricted. Due to a lack of negative-strand RNA it could not be established in this
262 assay whether synthesis of new positive-strand genomes requires the *cre*. However, given evidence
263 from the literature of the importance to positive-strand RNA synthesis, these findings would suggest
264 that the c*re* is essential for efficient priming of replication by $3D^{pol}$ in the infected cell.

265 In conclusion, we present a method using 5-EU labelling and purification of nascent RNA prior to
266 strand-specific qPCR that can be applied to determine the role of viral elements in transcription of
267 positive- and negative-strands using replicons containing specific mutations. Here, this was applied to
268 the known c*re* mutations A1G and Δc*re* and showed that neither are capable of producing a negative-
269 strand intermediate. We will continue to probe other mutants in order to discover the role of viral
270 elements that control viral replication of positive- and negative-strands.

271 **Funding information**
272

273 This project was funded by the Biotechnology and Biological Sciences Research council UK (project
274 grant reference BB/T015748/1).

275

276 **Acknowledgements**
277

278 We are grateful to group members for their helpful comments on the project.

279

280 **Author contributions**
281

The project was conceived by the authors. The experiments were carried out and the data analysed by SJD. The manuscript was drafted by SJD and was edited and revised by all authors.

Conflicts of interest

The authors declare that there are no conflicts of interest.

References

1. Paton DJ, Di Nardo A, Knowles NJ, Wadsworth J, Pituco EM, Cosivi O, et al. The history of foot-and-mouth disease virus serotype C: the first known extinct serotype? Virus Evol. 2021;7(1):veab009.

2. Jamal SM, Belsham GJ. Foot-and-mouth disease: past, present and future. Vet Res. 2013;44:116.

3. Knight-Jones TJ, Rushton J. The economic impacts of foot and mouth disease - what are they, how big are they and where do they occur? Prev Vet Med. 2013;112(3-4):161-73.

4. Feng S, Patton M, Davis J. Market Impact of Foot-and-Mouth Disease Control Strategies: A UK Case Study. Front Vet Sci. 2017;4:129.

5. Thompson D, Muriel P, Russell D, Osborne P, Bromley A, Rowland M, et al. Economic costs of the foot and mouth disease outbreak in the United Kingdom in 2001. Rev Sci Tech. 2002;21(3):675-87.

6. Mahapatra M, Parida S. Foot and mouth disease vaccine strain selection: current approaches and future perspectives. Expert Rev Vaccines. 2018;17(7):577-91.

7. Park JH. Requirements for improved vaccines against foot-and-mouth disease epidemics. Clin Exp Vaccine Res. 2013;2(1):8-18.

8. Stenfeldt C, Eschbaumer M, Rekant SI, Pacheco JM, Smoliga GR, Hartwig EJ, et al. The Foot-and-Mouth Disease Carrier State Divergence in Cattle. J Virol. 2016;90(14):6344-64.

9. Dawe PS, Sorensen K, Ferris NP, Barnett IT, Armstrong RM, Knowles NJ. Experimental transmission of foot-and-mouth disease virus from carrier African buffalo (Syncerus caffer) to cattle in Zimbabwe. Vet Rec. 1994;134(9):211-5.

10. Dawe PS, Flanagan FO, Madekurozwa RL, Sorensen KJ, Anderson EC, Foggin CM, et al. Natural transmission of foot-and-mouth disease virus from African buffalo (Syncerus caffer) to cattle in a wildlife area of Zimbabwe. Vet Rec. 1994;134(10):230-2.

11. Gao Y, Sun SQ, Guo HC. Biological function of Foot-and-mouth disease virus non-structural proteins and non-coding elements. Virol J. 2016;13:107.

12. Roberts PJ, Belsham GJ. Identification of critical amino acids within the foot-and-mouth disease virus leader protein, a cysteine protease. Virology. 1995;213(1):140-6.

13. Vakharia VN, Devaney MA, Moore DM, Dunn JJ, Grubman MJ. Proteolytic processing of foot-and-mouth disease virus polyproteins expressed in a cell-free system from clone-derived transcripts. J Virol. 1987;61(10):3199-207.

14. Moffat K, Knox C, Howell G, Clark SJ, Yang H, Belsham GJ, et al. Inhibition of the secretory pathway by foot-and-mouth disease virus 2BC protein is reproduced by coexpression of 2B with 2C, and the site of inhibition is determined by the subcellular location of 2C. J Virol. 2007;81(3):1129-39.

322 15. Yost SA, Marcotrigiano J. Viral precursor polyproteins: keys of regulation from replication to
323 maturation. Curr Opin Virol. 2013;3(2):137-42.

324 16. Ferrer-Orta C, Arias A, Agudo R, Perez-Luque R, Escarmis C, Domingo E, et al. The structure of
325 a protein primer-polymerase complex in the initiation of genome replication. EMBO J. 2006;25(4):880-
326 8.

327 17. Birtley JR, Knox SR, Jaulent AM, Brick P, Leatherbarrow RJ, Curry S. Crystal structure of foot-
328 and-mouth disease virus 3C protease. New insights into catalytic mechanism and cleavage specificity.
329 J Biol Chem. 2005;280(12):11520-7.

330 18. Grubman MJ, Zellner M, Bablanian G, Mason PW, Piccone ME. Identification of the active-site
331 residues of the 3C proteinase of foot-and-mouth disease virus. Virology. 1995;213(2):581-9.

332 19. Forss S, Schaller H. A tandem repeat gene in a picornavirus. Nucleic Acids Res.
333 1982;10(20):6441-50.

334 20. King AM, Sangar DV, Harris TJ, Brown F. Heterogeneity of the genome-linked protein of foot-
335 and-mouth disease virus. J Virol. 1980;34(3):627-34.

336 21. Gonzalez-Magaldi M, Martin-Acebes MA, Kremer L, Sobrino F. Membrane topology and
337 cellular dynamics of foot-and-mouth disease virus 3A protein. PLoS One. 2014;9(9):e106685.

338 22. Ferrer-Orta C, Arias A, Perez-Luque R, Escarmis C, Domingo E, Verdaguer N. Structure of foot-
339 and-mouth disease virus RNA-dependent RNA polymerase and its complex with a template-primer
340 RNA. J Biol Chem. 2004;279(45):47212-21.

341 23. Herod MR, Gold S, Lasecka-Dykes L, Wright C, Ward JC, McLean TC, et al. Genetic economy in
342 picornaviruses: Foot-and-mouth disease virus replication exploits alternative precursor cleavage
343 pathways. PLoS Pathog. 2017;13(10):e1006666.

344 24. Ward JC, Lasecka-Dykes L, Neil C, Adeyemi OO, Gold S, McLean-Pell N, et al. The RNA
345 pseudoknots in foot-and-mouth disease virus are dispensable for genome replication, but essential
346 for the production of infectious virus. PLoS Pathog. 2022;18(6):e1010589.

347 25. Mason PW, Bezborodova SV, Henry TM. Identification and characterization of a cis-acting
348 replication element (cre) adjacent to the internal ribosome entry site of foot-and-mouth disease virus.
349 J Virol. 2002;76(19):9686-94.

350 26. Kanda T, Ozawa M, Tsukiyama-Kohara K. IRES-mediated translation of foot-and-mouth
351 disease virus (FMDV) in cultured cells derived from FMDV-susceptible and -insusceptible animals. BMC
352 Vet Res. 2016;12:66.

353 27. Kloc A, Diaz-San Segundo F, Schafer EA, Rai DK, Kenney M, de Los Santos T, et al. Foot-and-
354 mouth disease virus 5'-terminal S fragment is required for replication and modulation of the innate
355 immune response in host cells. Virology. 2017;512:132-43.

356 28. Carrillo C, Tulman ER, Delhon G, Lu Z, Carreno A, Vagnozzi A, et al. Comparative genomics of
357 foot-and-mouth disease virus. J Virol. 2005;79(10):6487-504.

358 29. Lopez de Quinto S, Martinez-Salas E. Conserved structural motifs located in distal loops of
359 aphthovirus internal ribosome entry site domain 3 are required for internal initiation of translation. J
360 Virol. 1997;71(5):4171-5.

361 30. Lopez de Quinto S, Saiz M, de la Morena D, Sobrino F, Martinez-Salas E. IRES-driven translation
362 is stimulated separately by the FMDV 3'-NCR and poly(A) sequences. Nucleic Acids Res.
363 2002;30(20):4398-405.

364 31. Xiang W, Harris KS, Alexander L, Wimmer E. Interaction between the 5'-terminal cloverleaf
365 and 3AB/3CDpro of poliovirus is essential for RNA replication. J Virol. 1995;69(6):3658-67.

366 32. Gamarnik AV, Andino R. Interactions of viral protein 3CD and poly(rC) binding protein with the
367 5' untranslated region of the poliovirus genome. J Virol. 2000;74(5):2219-26.

368 33. Harris KS, Xiang W, Alexander L, Lane WS, Paul AV, Wimmer E. Interaction of poliovirus
369 polypeptide 3CDpro with the 5' and 3' termini of the poliovirus genome. Identification of viral and
370 cellular cofactors needed for efficient binding. J Biol Chem. 1994;269(43):27004-14.

371 34. Yang Y, Rijnbrand R, Watowich S, Lemon SM. Genetic evidence for an interaction between a
372 picornaviral cis-acting RNA replication element and 3CD protein. J Biol Chem. 2004;279(13):12659-67.

373 35. Yang F, Zhu Z, Cao W, Liu H, Wei T, Zheng M, et al. Genetic Determinants of Altered Virulence
374 of Type O Foot-and-Mouth Disease Virus. J Virol. 2020;94(7).

375 36. Kloc A, Rai DK, Rieder E. The Roles of Picornavirus Untranslated Regions in Infection and Innate
376 Immunity. Front Microbiol. 2018;9:485.

377 37. Zhu Z, Yang F, Cao W, Liu H, Zhang K, Tian H, et al. The Pseudoknot Region of the 5'
378 Untranslated Region Is a Determinant of Viral Tropism and Virulence of Foot-and-Mouth Disease Virus.
379 J Virol. 2019;93(8).

380 38. Mohapatra JK, Pawar SS, Tosh C, Subramaniam S, Palsamy R, Sanyal A, et al. Genetic
381 characterization of vaccine and field strains of serotype A foot-and-mouth disease virus from India.
382 Acta Virol. 2011;55(4):349-52.

383 39. Escarmis C, Dopazo J, Davila M, Palma EL, Domingo E. Large deletions in the 5'-untranslated
384 region of foot-and-mouth disease virus of serotype C. Virus Res. 1995;35(2):155-67.

385 40. Paul AV, Rieder E, Kim DW, van Boom JH, Wimmer E. Identification of an RNA hairpin in
386 poliovirus RNA that serves as the primary template in the in vitro uridylylation of VPg. J Virol.
387 2000;74(22):10359-70.

388 41. Nayak A, Goodfellow IG, Belsham GJ. Factors required for the Uridylylation of the foot-and-
389 mouth disease virus 3B1, 3B2, and 3B3 peptides by the RNA-dependent RNA polymerase (3Dpol) in
390 vitro. J Virol. 2005;79(12):7698-706.

391 42. Schein CH, Ye M, Paul AV, Oberste MS, Chapman N, van der Heden van Noort GJ, et al.
392 Sequence specificity for uridylylation of the viral peptide linked to the genome (VPg) of enteroviruses.
393 Virology. 2015;484:80-5.

394 43. Paul AV, Yin J, Mugavero J, Rieder E, Liu Y, Wimmer E. A "slide-back" mechanism for the
395 initiation of protein-primed RNA synthesis by the RNA polymerase of poliovirus. J Biol Chem.
396 2003;278(45):43951-60.

397 44. Paul AV, Peters J, Mugavero J, Yin J, van Boom JH, Wimmer E. Biochemical and genetic studies
398 of the VPg uridylylation reaction catalyzed by the RNA polymerase of poliovirus. J Virol.
399 2003;77(2):891-904.

400 45. Paul AV, van Boom JH, Filippov D, Wimmer E. Protein-primed RNA synthesis by purified
401 poliovirus RNA polymerase. Nature. 1998;393(6682):280-4.

402 46. Belsham GJ, Brangwyn JK. A region of the 5' noncoding region of foot-and-mouth disease virus
403 RNA directs efficient internal initiation of protein synthesis within cells: involvement with the role of
404 L protease in translational control. J Virol. 1990;64(11):5389-95.

405 47. Bienz K, Egger D, Pfister T, Troxler M. Structural and functional characterization of the
406 poliovirus replication complex. J Virol. 1992;66(5):2740-7.

407 48. Lundquist RE, Maizel JV, Jr. In vivo regulation of the poliovirus RNA polymerase. Virology.
408 1978;89(2):484-93.

409 49. Barton DJ, Flanegan JB. Synchronous replication of poliovirus RNA: initiation of negative-
410 strand RNA synthesis requires the guanidine-inhibited activity of protein 2C. J Virol. 1997;71(11):8482-
411 9.

412 50. Richards OC, Martin SC, Jense HG, Ehrenfeld E. Structure of poliovirus replicative intermediate
413 RNA. Electron microscope analysis of RNA cross-linked in vivo with psoralen derivative. J Mol Biol.
414 1984;173(3):325-40.

415 51. Triantafilou K, Vakakis E, Kar S, Richer E, Evans GL, Triantafilou M. Visualisation of direct
416 interaction of MDA5 and the dsRNA replicative intermediate form of positive strand RNA viruses. J Cell
417 Sci. 2012;125(Pt 20):4761-9.

418 52. Goodfellow IG, Polacek C, Andino R, Evans DJ. The poliovirus 2C cis-acting replication element-
419 mediated uridylylation of VPg is not required for synthesis of negative-sense genomes. J Gen Virol.
420 2003;84(Pt 9):2359-63.

421 53. Morasco BJ, Sharma N, Parilla J, Flanegan JB. Poliovirus cre(2C)-dependent synthesis of
422 VPgpUpU is required for positive- but not negative-strand RNA synthesis. J Virol. 2003;77(9):5136-44.

423 54. Murray KE, Barton DJ. Poliovirus CRE-dependent VPg uridylylation is required for positive-
424 strand RNA synthesis but not for negative-strand RNA synthesis. J Virol. 2003;77(8):4739-50.

425 55. Horsington J, Zhang Z. Analysis of foot-and-mouth disease virus replication using strand-
426 specific quantitative RT-PCR. J Virol Methods. 2007;144(1-2):149-55.

427 56. Plaskon NE, Adelman ZN, Myles KM. Accurate strand-specific quantification of viral RNA. PLoS
428 One. 2009;4(10):e7468.

429 57. Tuiskunen A, Leparc-Goffart I, Boubis L, Monteil V, Klingstrom J, Tolou HJ, et al. Self-priming
430 of reverse transcriptase impairs strand-specific detection of dengue virus RNA. J Gen Virol. 2010;91(Pt
431 4):1019-27.

432 58. Vashist S, Urena L, Goodfellow I. Development of a strand specific real-time RT-qPCR assay for
433 the detection and quantitation of murine norovirus RNA. J Virol Methods. 2012;184(1-2):69-76.

434 59. Muller M, Slivinski N, Todd E, Khalid H, Li R, Karwatka M, et al. Chikungunya virus requires
435 cellular chloride channels for efficient genome replication. PLoS Negl Trop Dis. 2019;13(9):e0007703.

436 60. Tulloch F, Pathania U, Luke GA, Nicholson J, Stonehouse NJ, Rowlands DJ, et al. FMDV replicons
437 encoding green fluorescent protein are replication competent. J Virol Methods. 2014;209:35-40.

438 61. Herod MR, Loundras EA, Ward JC, Tulloch F, Rowlands DJ, Stonehouse NJ. Employing
439 transposon mutagenesis to investigate foot-and-mouth disease virus replication. J Gen Virol.
440 2015;96(12):3507-18.

441 62. Steil BP, Barton DJ. Cis-active RNA elements (CREs) and picornavirus RNA replication. Virus
442 Res. 2009;139(2):240-52.

443

444 ## Figure legends

445 **Figure 1: Transfection of FMDV replicon RNA is not compatible with distinguishing the synthesis of**
446 **positive and negative strand molecules during replication.** (A) Schematic overview of a replicon
447 transfection assay with imaging prior to RNA extraction, cDNA synthesis and strand-specific qPCR. (B)
448 Incucyte S3 imaging of BHK-21 cells transfected with WT and replication deficient $3D^{GNN}$ (GNN) FMDV
449 pRep-ptGFP RNA and yeast tRNA (as a control), with phase contrast and green visualisation over time.
450 Scale bar = 400 µm. (C) Detection over time of ptGFP following transfection with FMDV replicon RNA.
451 (D) Schematic representation of primer binding regions with P2 and P3 genomic regions of FMDV for
452 the cDNA synthesis and qPCR detection of positive- and negative-strands. RNA extracted from
453 transfected cells was reverse transcribed using strand-specific primers prior to qPCR to detect
454 positive-strand (E) and negative-strand (F) expression. Analysis was performed using the ΔΔCq method
455 relative to WT. Statistical analysis was performed by one-way ANOVA with ** *P*-value = *<0.005* and
456 **** *P*-value = *<0.0001*. n = 3.

457 **Figure 2: Removal of input replicon RNA by 5-EU labelling and RNA pulldown to select newly**
458 **synthesised RNA.** (A) Schematic representation of a 5-EU nascent RNA labelling assay. BHK cells were
459 transfected with FMDV pRep-ptGFP RNA (WT and GNN), with addition of 0.2 mM 5-EU to label nascent
460 RNA. An unlabelled control was also included (termed WT no EU). Cells were imaged using an Incucyte
461 S3 instrument prior to harvesting of RNA 6 hours post transfection. 5-EU labelled RNA was biotinylated
462 by click reaction and captured with streptavidin magnetic beads. Input RNA was removed by washing
463 prior to on-bead cDNA synthesis and strand-specific qPCR. (B) ptGFP positive cells detected by
464 Incucyte S3 imaging 6 hours post transfection to determine effect of 5-EU labelling on replication.
465 Following RNA extraction, strand-specific qPCR to detect positive-strands (C) and negative-strands (D)
466 prior to click reaction, was performed. Click reaction mediated biotinylation of nascent RNA, magnetic
467 bead capture and on bead cDNA synthesis was performed prior to strand-specific assays to determine
468 positive-strand (E) and negative-strand (F) expression. Analysis was performed using the ΔΔCq method
469 relative to WT. Statistical analysis was performed by one-way ANOVA with ** *P*-value = *<0.005* and
470 **** *P*-value = *<0.0001*. n = 3.

471 **Figure 3: FMDV *cre* is essential to the production of negative-strand genomes.** (A) BHK-21 cells were
472 transfected with pRep-ptGFP constructs containing *cre* mutations A1G and Δ*cre* (alongside WT and
473 GNN controls as described in Figure 1) with addition of 0.2 mM 5-EU to label nascent transcribed RNA.
474 ptGFP positive cells were visualised 6 hours post-transfection using an Incucyte S3 instrument. Total
475 RNA extracted 6 hours post transfection was biotinylated by click reaction, captured with streptavidin
476 beads and reverse transcribed using strand-specific or oligo $dT_{(20)}$ as a primer. cDNA was used in

477 strand-specific qPCR assays to determine positive-strand (B) and negative-strand (C) expression.
478 Analysis was performed using the ΔΔCq method relative to WT. Statistical analysis was performed by
479 one-way ANOVA with **** *P*-value = *<0.0001*. n = 3.

480 ## Tables and figures

481

Table 1: Primers used in RT and qPCR reactions. Underlined are the non-viral tag sequences for both the RT and qPCR primers.

Target	Application	Name	Sequence (5'-3')
Positive-strand	RT	PS-tag-RT	GCAGGAGCTAAGCGCTGGGGTCGCGATGATGACTTTGC
	qPCR	PS-qPCR-TAG	GCAGGAGCTAAGCGCTGG
	qPCR	PS-qPCR-R	GATTTGGGCCAGAACCCTGA
Negative-strand	RT	NS-tag-RT	TGACGTTGCGACGAGTTCGCCAAAGACGGAGCTGACACT
	qPCR	NS-qPCR-TAG	TGACGTTGCGACGAGTTCG
	qPCR	NS-qPCR-R	GTCCACAATCAACCCCTCGT
β-actin	qPCR	β-actin-F	GTGCTATGTTGCCCTGGACT
	qPCR	β-actin-R	GCTCGTTGCCAATGGTGATG

482 **Figure 1**

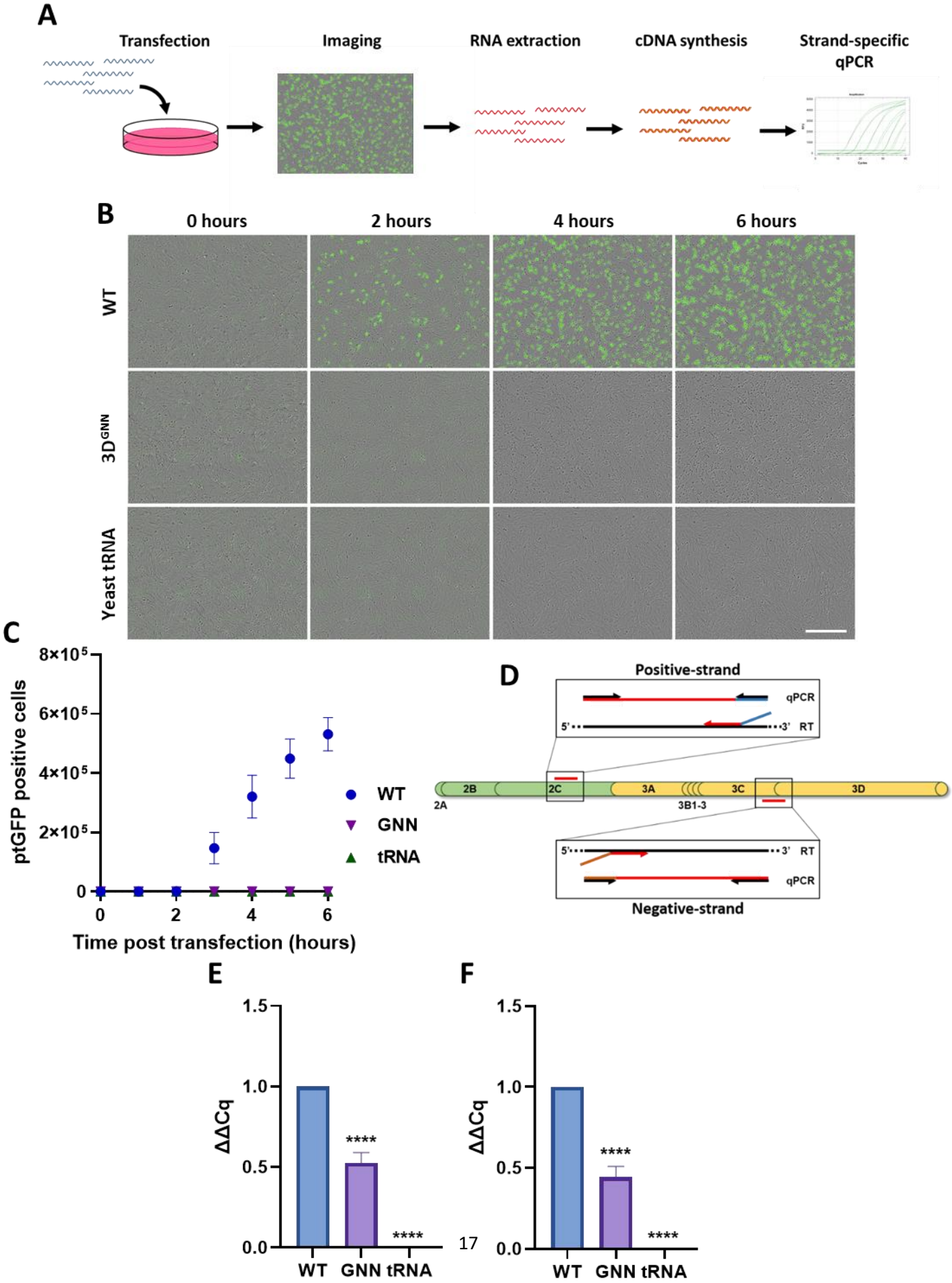
A
Transfection
Imaging
RNA extraction
cDNA synthesis
Strand-specific qPCR
B
0 hours
2 hours
4 hours
6 hours
WT
3D^GNN
Yeast tRNA
C
ptGFP positive cells
8×10^5
6×10^5
4×10^5
2×10^5
0
0
2
4
6
Time post transfection (hours)
WT
GNN
tRNA
D
Positive-strand
qPCR
5'
3'
RT
2A
2B
2C
3A
3B1-3
3C
3D
Negative-strand
E
F
ΔΔCq
1.5
1.0
0.5
0.0
****
WT
GNN
tRNA

Figure 2

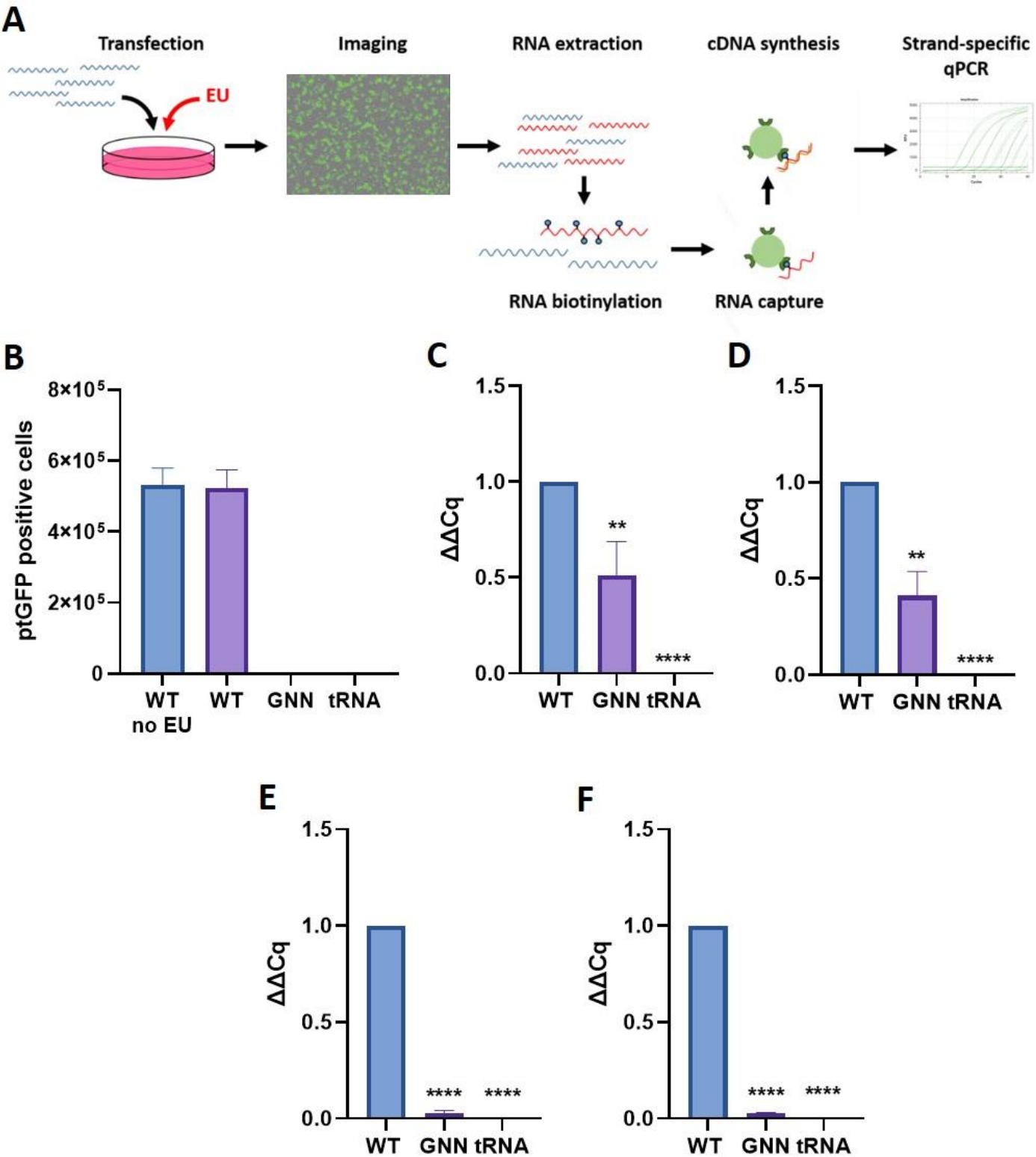
A
Transfection
EU
Imaging
RNA extraction
cDNA synthesis
Strand-specific qPCR
RNA biotinylation
RNA capture
B
ptGFP positive cells
8×10⁵
6×10⁵
4×10⁵
2×10⁵
0
WT no EU
WT
GNN
tRNA
C
ΔΔCq
1.5
1.0
0.5
0.0
**
****
WT
GNN
tRNA
D
ΔΔCq
1.5
1.0
0.5
0.0
**
****
WT
GNN
tRNA
E
ΔΔCq
1.5
1.0
0.5
0.0
****
****
WT
GNN
tRNA
F
ΔΔCq
1.5
1.0
0.5
0.0
****
****
WT
GNN
tRNA

483

Figure 3

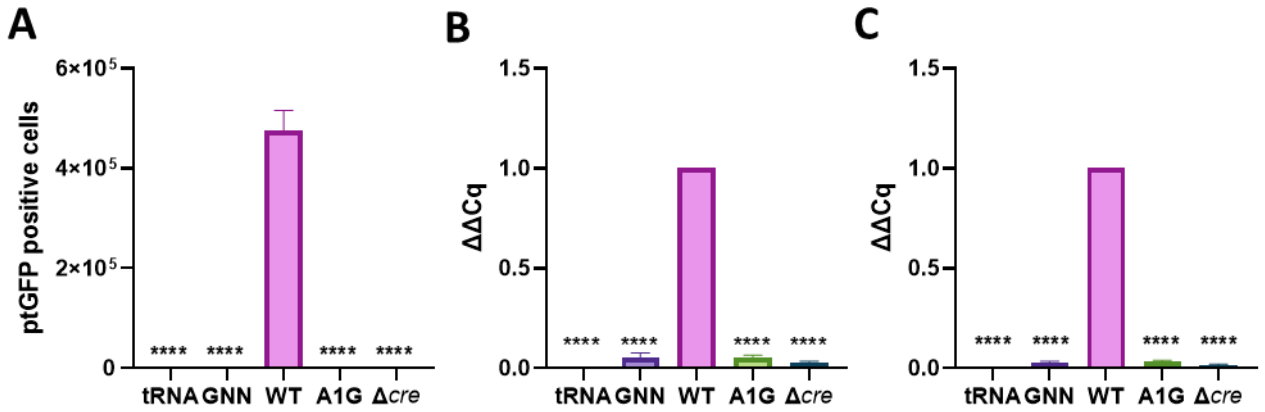
A
B
C
ptGFP positive cells
6×10^5
4×10^5
2×10^5
0
ΔΔCq
1.5
1.0
0.5
0.0
****
tRNA
GNN
WT
A1G
Δcre

484